High-Efficiency Bridgeless PFC Battery Charger for On-Board LEV PV Systems

MADDELA TRISHA [1] | D.MOUNIKA[2]

[1]Pg Scholar, Dept of EPS, Kodada Institute of Technology & Science for Women-Kodad, Telangana.

[2] Assistant Professor, Dept of EEE, Kodada Institute of Technology & Science for Women-Kodad,Telangana.

ABSTRACT: This study presents a bridgeless single-stage power factor correction (PFC) Cuk converter–based electric vehicle (EV) charger employing a fractional-order proportional–integral (FOPI) controller. Many existing EV chargers use multistage converter architectures to achieve unity power factor and low grid current harmonics. However, these multistage systems require many semiconductor switches, which increases conduction losses, cost, and system complexity. Furthermore, conventional chargers typically support grid-only operation. To overcome these limitations and enable dual-source operation with both the utility grid and a photovoltaic (PV) module, a single-stage bridgeless PFC Cuk converter is proposed. The developed topology utilizes an optimized number of switches and energy storage components to efficiently charge the EV battery. An outer control loop based on the FOPI control strategy is implemented to regulate the battery charging current while simultaneously improving grid-side power factor. The FOPI controller introduces an additional fractional-order parameter, providing greater tuning flexibility and enhanced dynamic performance compared to conventional PI controllers. As a result, the grid current exhibits reduced harmonic distortion, particularly under light-load and dual-input operating conditions, where traditional PI-based PFC controllers tend to show degraded performance. The improved damping characteristics and robustness of the FOPI controller also ensure stable operation during disturbances such as PV intermittency, grid voltage disturbances, thereby enhancing power quality and system reliability. Therefore, the proposed FOPI-based control scheme plays a vital role in achieving unity power factor operation, robust dynamic response, and smooth

regulation of battery voltage and current under varying PV and grid conditions.

KEYWORDS: PFC, CUK CONVERTER, SOLAR, POWER FACTOR, HARMONICS.

I.INTRODUCTION: THE increasing popularity and appeal of mild electric powered automobiles (LEVs) with a photovoltaic (PV) panel placed atop the automobile, specially in growing international locations which includes India, has opened up new studies paths. Electric automobile (EV) charging structures are one of the maximum energetic studies topics. For completely grid-structured EVs, several electricity thing-corrected (PFC) chargers have been proposed all through the past few a long time. Interestingly, those setups are classified according to their structure as both single-level or two-level chargers. Core premise of a PFC charger is to deliver a ripple-unfastened current to battery at the same time as additionally keeping a high strength issue at the enter. For -stage topologies to do both duties, two converters (ac–dc and dc–dc) are required. In one-degree charging, but, each tasks are performed with the aid of a single ac–dc interface converter. It now has the inherent advantages of a more straightforward shape and increased effectiveness [1-7]. In a -degree onboard charger, galvanic isolation is usually used by adding an isolated dc–dc converter to the second stage. However, SAE J1772 widespread does not necessitate the employment of transformers as a protection requirement for EVs. Furthermore, isolation with grid enter is not required because battery ground is constantly in a floating state with a vehicle's chassis [8], [9], and [10]. For protection precautions, the large transformer can be swapped out for small, cheap relay circuits [10]. Additionally, due to leakage inductance, including transformers to isolated topologies results in accelerated size, losses, complexity, and switch stress. As a result, nonisolated single-degree topologies are gaining traction as low cost LEV charging alternatives.

In fashionable, increase converter-based totally PFC architecture is widely used for grid enter sinusoid current shaping [11]. However, due to output voltages extra than the grid voltage peak, its use for single-level low-voltage charging programs is confined. Other topologies with greenback-increase competencies, such Cuk, SEPIC, and Zeta, are terrific picks for such programs in order to overcome those issues [12]. Among the aforementioned possibilities, Cuk converterderived topologies provide diverse benefits, which includes native protection towards inrush present day and providing non-stop cutting-edge at enter and output. A diode-bridged rectifier (DBR) is cascaded with a Cuk converter to create a conventional bridged Cuk rectifier [13]. Conduction losses in DBR, however, have a bad impact on charger efficiency.

To boom efficiency, some of bridgeless Cuk topologies have been counseled as substitutes for bridged Cuk topologies. The PFC rectifier that is being proven does no longer require a bridge since it makes use of two Cuk circuits, each of which operates in an opportunity voltage polarity. It decreases every issue's intake whilst increasing the range of components. By the usage of a common Cuk circuit for each superb and poor voltage polarity, work has decreased the quantity of components. To lessen the scale of the output capacitor, a novel manage method is used. Higher performance also comes at the fee of a further regulated transfer. We introduce a bridgeless Cuk PFC topology with tender switching for full voltage and cargo capability. Although it will increase performance and lowers switching and conduction losses, the application of soft switching necessitates extra semiconductor devices and passive components. Nevertheless, grid input is the only way for these single-level bridgeless PFC topologies to rate. Consequently, an additional dc-dc converter would be needed for the most strength point tracking (MPPT) of a PV panel integrated with LEV.

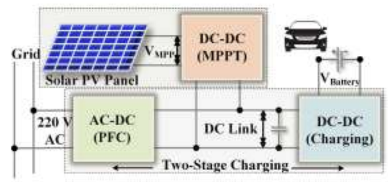

Fig. 1. Conventional solar PV incorporated PFC charging system.

Fig. 1 shows a block schematic of traditional charging topologies for dual enter assets that consist of each grid and PV panel input. It is clear that to be able to acquire the essential charging configuration, three converters are used. Here, an ac-dc converter handles energy aspect correction, a dc-dc converter on the PV panel quit handles MPPT, and any other dc-dc converter is used for battery charging. This type of setup is pretty regular for high power output. It, however, needs a massive number of switching and magnetic components. To remedy this problem, a extraordinary configuration that does not require a dc–dc converter to accomplish the MPPT is proposed. In this case, a PV panel is delivered immediately throughout the DC hyperlink with out the want for an interface converter. However, the PV panel wishes to be built to run at a higher voltage on the maximum power factor (MPP) because the PFC converter is strolling in increase mode on this setup. Using a multiport charger is every other manner to integrate severa sources even as minimizing the quantity of components. Both the AC mains and PV panels may be used to rate EVs. By using a single power converter for all sports, it lowers costs and will increase performance. It can best use one power supply at a time, although. A single-stage power conversion is achieved the usage of a multiport PFC charger that is based totally on a Z-source inverter. Nevertheless, a greater range of switching additives are wished. It is rare to find a multi-enter PFC charger with fewer components that may use all assets each one by one and concurrently.

II.PROPOSED SYSTEM: A Cuk-derived bridgeless dual-input LEV charger is shown in Fig. 2 to solve the above mentioned problems. In this case, the PV panel is the secondary input and the grid is the primary input. The unique qualities of this charger and the contributions of this effort are described below.

1) Compared to traditional DBR-based ac–dc chargers, the presented charger's bridgeless architecture at grid input reduces losses.

2) It also benefits from nonpulsating currents at each port because it is built on a Cuk converter. 3) Additionally, single-stage power conversion and component sharing between two sources guarantee a decrease in the overall number of components.

4) In addition, a PV panel attached to the secondary input improves the grid current's power quality (PQ), a feature that is generally absent from conventional PV and grid-assisted battery charging systems. Measurements of the grid current's total harmonic distortion (THD), especially at lower power levels, verify this.

5) This charger enables both sources to operate simultaneously and independently, unlike a few reported integrated multiport PFC chargers.

6) Adding a high frequency transformer makes it simple to include isolation.

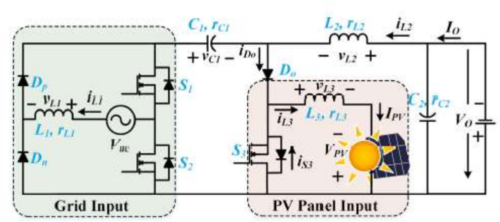

Fig. 2. Schematic of bridgeless LEV charger.

The bridgeless multiport PFC charger discussed in this article inherits the merits of a standard Cuk PFC rectifier and follows a similar operating concept. Additionally, PV panel input can be added by changing a typical two-port Cuk converter. The redesigned topology shown here comprises three inductors and two capacitors and is depicted in Fig. 2. It also involves the employment of three switches and three diodes. Here, two switches, S1 and S2, are utilised in place of two DBR diodes to build a bridgeless architecture for ac input. Diode Dp conducts when the voltage polarity is positive, while diode Dn conducts when the voltage polarity is negative. The primary input's instantaneous sinusoidal grid voltage is expressed as:

$$V_{\mathrm{ac}}(t) = V_p \sin(314t).$$

Vp stands for the peak value of Vac(t) in the equation above. Vac(t) can be taken to be constant and stated as Vac in a single switching cycle because switching frequency is comparatively high when compared to grid frequency. Similarly, DS1 and DS2 in a switching period can be used to represent time-varying duties DS1(t) and DS2(t) of grid input and PV input, respectively. Switches S1 and S2 are controlled by DS1. Meanwhile, switch S3 is operated by DS2 in tandem with other two switches to perform the MPPT of PV panel input. Depending on the availability of each source, the charger can function in three different charging states: dual input charging, grid charging, and PV stand-alone charging.

A. Dual Input Charging Batteries are charged by dual input charging, which uses inputs from both the grid and the photovoltaic system. Three modes of operation are used to demonstrate the operation of the charger during a single switching cycle for grid-PV charging. Fig. 3(a) shows the logic used to generate control pulses for each mode. The durations of modes 1, 2, and 3 are denoted by d1, d2, and d3, accordingly. Fig. 3(b)–(d) depicts the charger's operation for positive voltage polarity. Likewise, Fig. 3(e)–(g) demonstrates its operation for negative polarity. Switches S1 and S2 conduct in modes 1 and 3, whereas S3 conducts in mode 3..

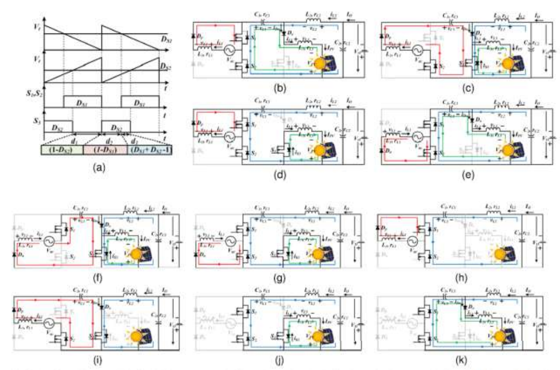

Fig. 3. (a) Pictorial representation of switching pulse generation for each operational mode. Equivalent circuit representation (b)–(d) dual input charging in positive voltage polarity, (e)–(g) dual input charging in negative voltage polarity, (h) and (i) grid charging, and (j) and (k) PV stand-alone charging.

Mode-1: In mode 1, grid charges input inductor L1. Since Dn is reverse biased when voltage is positive, and iL1 flows through Dp. Conversely, iL1 passes through Dn when the voltage polarity is negative. In this condition, output inductor L2 is charged by C1. Inductor L3 discharges through C1 at PV input.

Mode-2: During positive voltage polarity, iL1 flows from diode Dp and switch S2, causing L1 to discharge. In a similar vein, voltage flows via S1 and Dn when it is negative. In the meantime, S3 is activated, allowing PV panel input to charge L3. In this mode, the other two inductors, L1 and L2, discharge in all voltage polarities.

Mode-3: In this mode, iL1 and iL2 can follow the same path as in the first mode since the switching states of S1 and S2 are the same as in mode 1. The only distinction is that inductor L3 is charged when switch S3 is turned on in mode 3. Voltage-second balancing of each inductor yields the voltage conversion ratio of output to each input, which may be expressed as

$$\frac{V_o}{V_{ac}} = \frac{D_{S1}}{1 - D_{S1}} \text{ and } \frac{V_o}{V_{PV}} = \frac{D_{S1}}{1 - D_{S2}}. \quad (2)$$

For a large load range, the switch current iS3 is negative at the beginning of mode 2 and turns positive in mode 3. At the beginning of mode 2, its magnitude is large enough to discharge S3's output capacitance and give the zero voltage switching (ZVS) condition for the same across a broad load range. For ZVS turn-on of S3, a fixed turn-on delay solution is used due to its ease of implementation.

B. Grid Charging Power transfer occurs in two modes of operation because the proposed converter's grid charging is comparable to that of a traditional PFC Cuk charger. The converter's operation in modes 1 and 2 is shown in Figs. 3(h) and (i), respectively. While conducting S3 in both modes, switches S1 and S2 are switched on and off in modes 1 and 2, respectively. Furthermore, in mode 1, inductors L1 and L2 are charged and C1 is discharged. Likewise, in mode 2, C1 charges while L1 and L2 discharge.

C. PV Stand-Alone Charging Even when driving or parked by the side of the road, the converter that is being offered may capture solar energy. It is displayed in Fig. 3(j) and (k) and is known as PV stand-alone charging. PV panels use an intermediary capacitor to transport their energy to the output. Nevertheless, it only operates in two modes, conducting S1 and S2 continuously while switching S3 in each mode. Fig. 3(k) depicts the circuit arrangement in mode 2. In mode 2, switch S3 is turned off.

TABLE I
SYSTEM SPECIFICATIONS

Specifications	Parameters	Value (Range)
AC Mains	Voltage (V_{ac})	110 V (90 V-130 V)
	Power (P_{ac})	470 W (P_{max} = 570 W)
PV Panel	Voltage at MPP (V_{pv})	40 V
	Power at MPP (P_{pv})	121.48 W
Output	Voltage (V_o)	72V (63 V-87 V)
	Power (P_o)	470 W (P_{max} = 570 W)
Switching Freq.	-	20 kHz

This section contains the design equations of the provided charger. The charger is intended to function in continuous conduction mode (CCM) according to the system parameters given in Table I. The charger's output voltage varies from 63 (Vo,min) to 87 V (Vo,max), where a lower level denotes a fully depleted battery and a higher voltage denotes a fully charged battery. The charger's output power fluctuates significantly and roughly linearly with the output voltage. It is designed to withstand sudden drops in grid voltage [down to 90 V (Vac,min)] and increases [up to 130 V (Vac,max)]. Therefore, every inductor and capacitor should be made to function in CCM for all necessary working conditions [(Vac,min, Vo,min), (Vac,min, Vo,max), (Vac,max, Vo,min), (Vac,max, Vo,max)].

A. Design of L1, L2, and L3 in CCM The input inductor (L1) has a significant impact on input current THD. As a result, it is made to reduce current ripple in all working conditions. It is noteworthy that when grid voltage reaches its maximum, the critical value of L1 is attained. The design equation for the same is provided as

$$L_1 = \frac{D_{S1}}{\gamma_{L1} f_s} \frac{V_{ac}^2}{P_{ac}} = \frac{V_{ac,max}^2}{\gamma_{L1} f_s} \frac{V_{o,max}/P_{ac,max}}{V_{o,max} + \sqrt{2} V_{ac,max}}. \quad (3)$$

With an 8% current ripple (γL1) at input, the computed value of L1 from (3) is 6.0 mH, which is also the value selected for prototype development. The formula for calculating L2 can be expressed as

$$L_2 = \frac{1 - D_{S1}}{\gamma_{L2} f_s} \frac{V_o}{i_{L2}} = \frac{V_{o,max}}{\gamma_{L2} f_s i_{L2}} \frac{\sqrt{2} V_{ac,max}}{V_{o,max} + \sqrt{2} V_{ac,max}}. \quad (4)$$

Notably, at maximum output voltage and peak grid voltage, an ideal value of L2 is reached. The relationship between it and the current (iL2) passing through it is inverse. The instantaneous value of (iL2) under certain conditions can be calculated using the following equation (Vac,max and Vo,max):

$$i_{L2}(t) = \frac{P_{ac} - P_{ac}\cos(2\omega t)}{V_o} = \frac{2P_{ac,max}}{V_{o,max}}. \quad (5)$$

The expression for determining L_2 for an aforementioned critical circumstances is as follows:

$$L_2 = \frac{V_{o,max}^2}{\gamma_{L2} f_s} \frac{((\sqrt{2} V_{ac,max})/(2P_{ac,max}))}{V_{o,max} + \sqrt{2} V_{ac,max}}. \quad (6)$$

The calculated and chosen value of L2 for 15% current ripple (γL2) is 1.5 mH. The input inductor (L3) at PV panel input is largely dictated by PV power, but it is also controlled by grid voltage since it effects duty ratio DS2. The critical value of L3 for a 12% current ripple (γL3) can be calculated using the following equation:

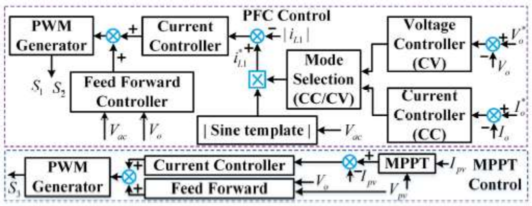

Fig. 4. Control strategy of bridgeless LEV charger.

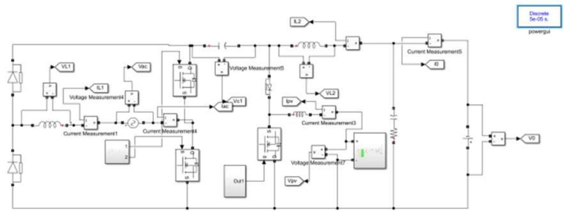

The main goal of the control architecture shown in Fig. 4 is to manage output current while executing maximum power tracking of PV panel input and sinusoidal shaping of grid current. Here, voltage mode MPPT control generates DS2 for switch S3, whereas current mode PFC control generates DS1 for switches S1 and S2. To create appropriate current compensators, the charger is subjected to small-signal analysis. Parasitic resistances of inductors (rL1, rL2, and rL3), ESR of capacitors (rC1 and rC2), and resistance of cable (Ro) connecting battery to the charger are all taken into consideration. State space variables include the voltage (vC1 and vC2) across capacitors and the currents (iL1, iL2, and iL3) passing through inductors. To create the necessary plant transfer function, state equations of the topology described for each operational mode are required.

III.SIMULATION RESULTS: Case1

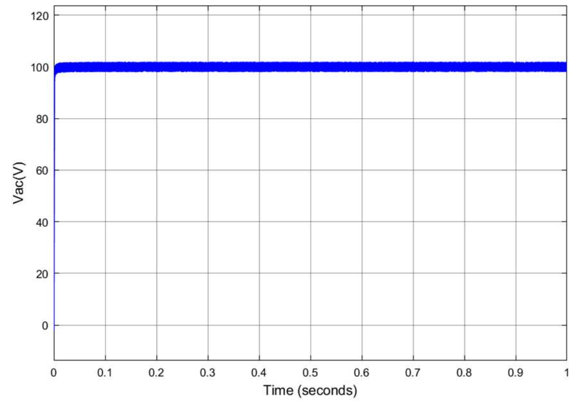

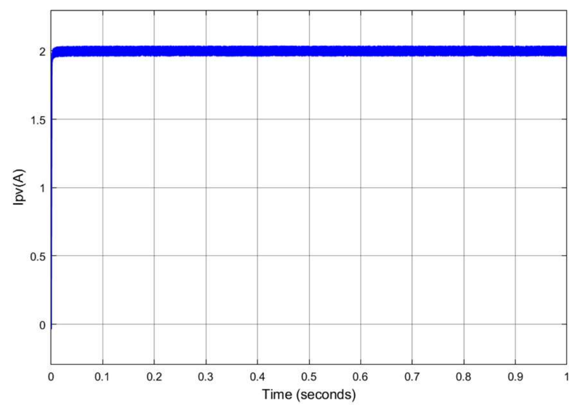

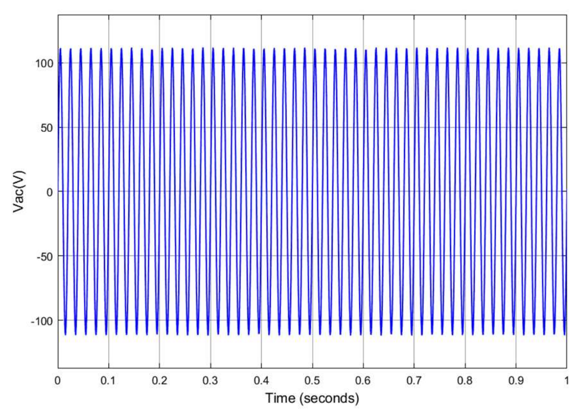

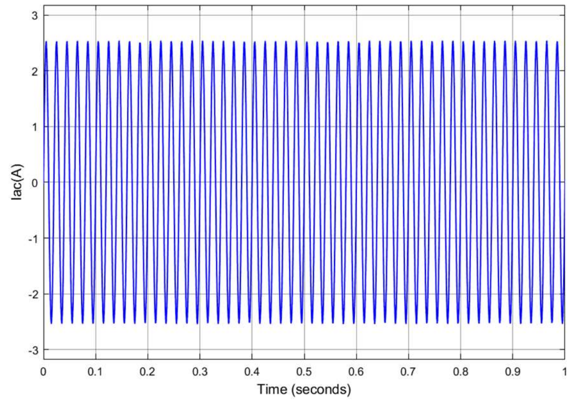

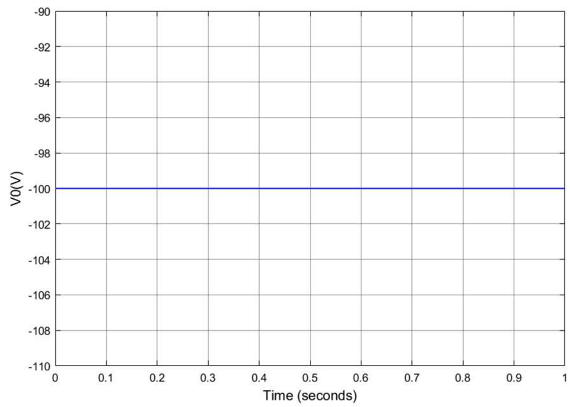

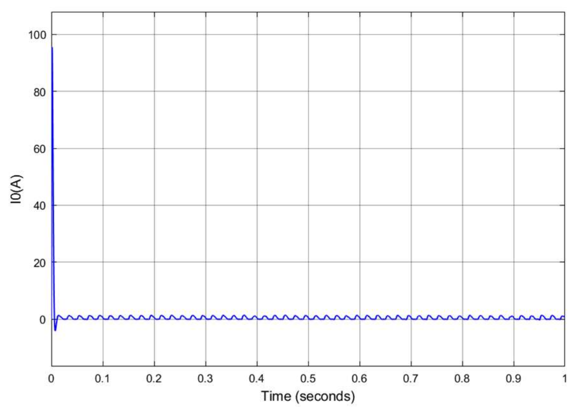

Case2

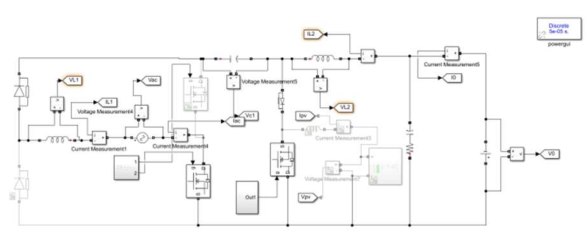

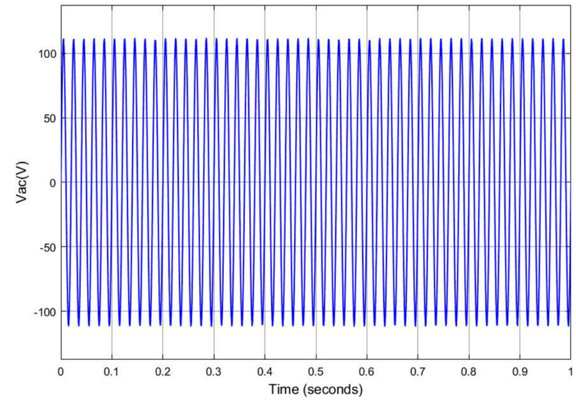

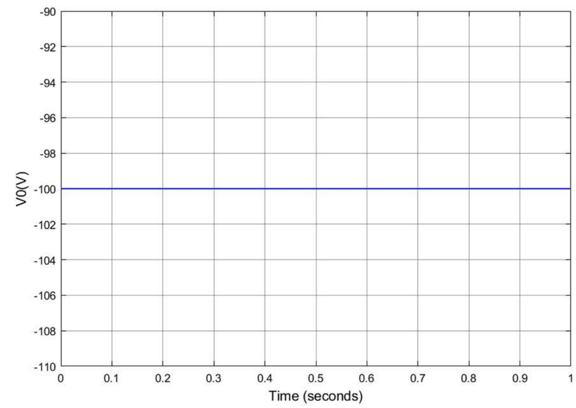

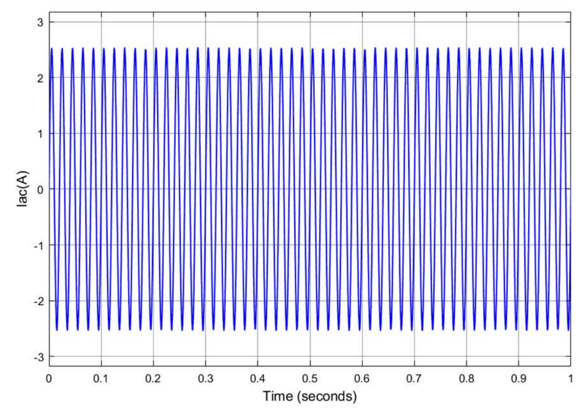

Case3 standalone

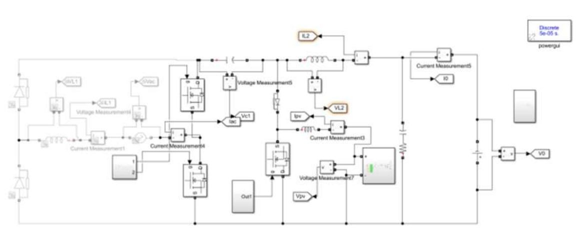

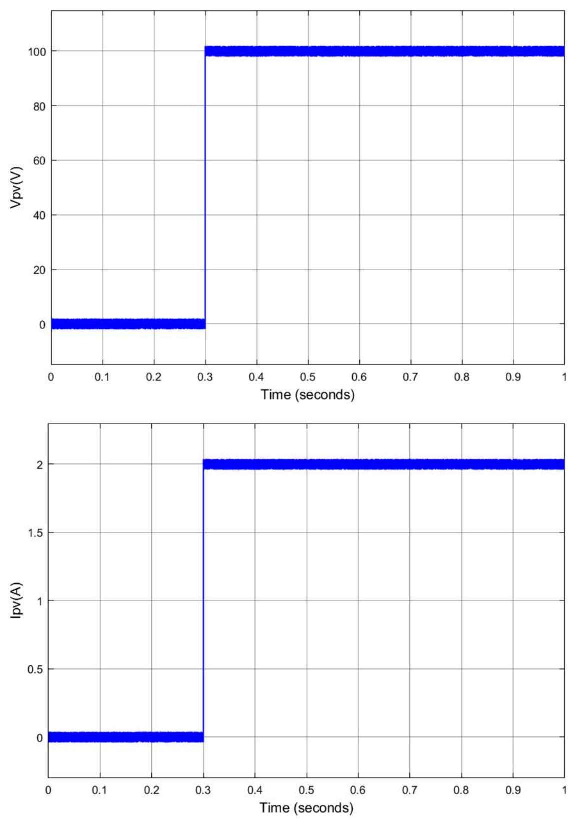

IV.CONCLUSION: This article presents a grid and PV panel interfaced charger for LEVs that has the advantage of better PQ of grid current. Both sources provide the dc output power, which can function both independently and concurrently. For the frequency response of the specified charger, a brief signal analysis is carried out and further validated by ac-sweep in PSIM. Under both steady-state and dynamic operating circumstances, it enhances the PQ of ac current and MPPT of PV panel input. Few components are shared between each source to reduce the overall components. Large filters are not required when there is an inductor at each input. By enhancing THD in grid current for dual input operation, the charger architecture offers an extra advantage over traditional topologies. By enhancing the voltage profile of the common intermediate capacitor between two sources, the addition of a PV panel lowers the THD in this case. The MATLAB/SIMULINK environment is used to verify the proposed topology's operation under both steady-state and various dynamic situations.

REFERENCES: [1] T.-T. Le, R. M. Hakim, and S. Choi, “A high-efficiency bidirectional single-stage AC–DC converter under wide voltage range for fast chargers,” IEEE Trans. Power Electron., vol. 38, no. 4, pp. 4945–4956, Apr. 2023.

[2] H. Nazi, E. Babaei, S. Tohidi, and M. Liserre, “An isolated SRC-based single phase single stage battery charger for electric vehicles,” IEEE Trans. Transport. Electrific., vol. 9, no. 1, pp. 1252–1262, Mar. 2023.

[3] H. Kim, J. Park, S. Kim, R. M. Hakim, H. Belkamel, and S. Choi, “A single-stage electrolytic capacitor-less EV charger with single- and three-phase compatibility,” IEEE Trans. Power Electron., vol. 37, no. 6, pp. 6780–6791, Jun. 2022.

[4] B. Vardani and N. R. Tummuru, “A single-stage bidirectional inductive power

transfer system with closed-loop current control strategy," IEEE Trans. Transport. Electrific., vol. 6, no. 3, pp. 948–957, Sep. 2020.

[5] S. R. Meher and R. K. Singh, "A standard two stage on-board charger with single controlled PWM and minimum switch count," IEEE Trans. Ind. Appl., vol. 59, no. 4, pp. 4628–4639, Jul./Aug. 2023.

[6] A. Singh, J. Gupta, and B. Singh, "Design and control of two stage battery charger for low voltage electric vehicles using high gain buck boost PFC AC–DC converter," IEEE Trans. Ind. Appl., vol. 59, no. 5, pp. 6125–6135, Sep./Oct. 2023.

[7] M. Tong, M. Cheng, S. Wang, and W. Hua, "An on-board two-stage integrated fast battery charger for EVs based on a five-phase hybrid excitation flux-switching machine," IEEE Trans. Ind. Electron., vol. 68, no. 2, pp. 1780–1790, Feb. 2021.

[8] C.-Y. Oh, D.-H. Kim, D.-G. Woo,W.-Y. Sung, Y.-S. Kim, and B.-K. Lee, "A high-efficient nonisolated single-stage on-board battery charger for electric vehicles," IEEE Trans. Power Electron., vol. 28, no. 12, pp. 5746–5757, Dec. 2013.

[9] A. V. J. S. Praneeth and S. S. Williamson, "Modeling, design, analysis, and control of a nonisolated universal on-board battery charger for electric transportation," IEEE Trans. Transport. Electrific., vol. 5, no. 4, pp. 912–924, Dec. 2019.

[10] J. Gupta and B. Singh, "A general purpose transformerless charging system based on fully bridgeless canonical switching cell high quality rectifier for LVEVs," IEEE Trans. Transport. Electrific., vol. 9, no. 3, pp. 4211–4222, Sep. 2023.